Preprint. Final version in
Proceedings Eighteenth IS&T Color Imaging Conference, San Antonio, Nov. 2010

XYZ to ADL: Calculating Logvinenko's Object Color Coordinates

Christoph Godau, Université Jean Monnet, Saint-Etienne, France
Brian Funt, Simon Fraser University, Vancouver, Canada

Abstract: Recently Logvinenko introduced a new object-color space, establishing a complete color atlas that is invariant to illumination [2]. However, the existing implementation for calculating the proposed color descriptors is computationally expensive and does not work for all types of illuminants. A new algorithm is presented that allows for an efficient calculation of Logvinenko's color descriptors for large data sets and a wide variety of illuminants.

Introduction

In the CIE XYZ space, colors of reflecting objects define a volume called the object-color solid [7, 2], which depends on the spectral power distribution of the illuminant. Figure 1 shows the object color solid for illuminant D65 in the CIE 1931 XYZ tristimulus space. Recently Logvinenko introduced a new object-color space, establishing a complete color atlas that is invariant to illumination [2], containing all colors in the object-color solid under any illuminant. However, Logvinenko's existing implementation for calculating the proposed color descriptors is computationally expensive and does not work for all types of illuminants.

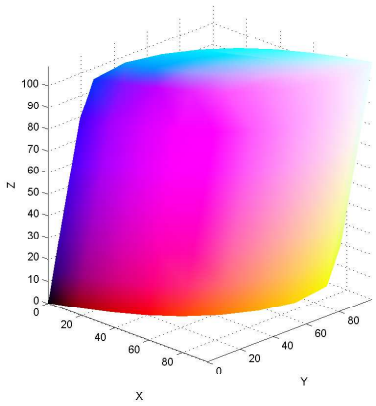

Figure 1: The object-color solid for illuminant D65 in the CIE 1931 XYZ space.

The points on the surface of the object-color solid are called optimal color stimuli, sometimes described as the object-color stimuli that for a given chromaticity have the greatest luminous reflectance [7]. It is generally accepted that they are generated by reflectance spectra that take values of either zero or one across the visible wavelength range, with no more than two transitions between these values, specified by transition wavelengths λ_1 and λ_2 [7]. There are two types of optimal reflectance functions, denoted $x_{opt}(\lambda;\lambda_1,\lambda_2)$. Type I functions take a value of one for $\lambda_1 < \lambda < \lambda_2$, and zero everywhere else, while Type II functions take a value of zero for $\lambda_2 < \lambda < \lambda_1$, and one everywhere else. Note that we follow Logvinenko's notation, where $\lambda_1 < \lambda_2$ for Type I and $\lambda_2 < \lambda_1$ for Type II reflectance functions.

It is also possible to describe the optimal reflectance functions using central wavelength, λ, and spectral bandwidth δ, to define the center and width of the interval described by the transition wavelengths. The central wavelength λ and spectral bandwidth δ can be calculated from the transition wavelengths as

$$\begin{aligned}\delta &= |\lambda_1 - \lambda_2| \\ \lambda &= \frac{\lambda_1 + \lambda_2}{2}\end{aligned}$$

for Type I optimal reflectances, and for Type II as

$$\begin{aligned}\delta &= (\lambda_{max} - \lambda_{min}) - |\lambda_1 - \lambda_2| \\ \lambda &= \begin{cases}\lambda_1 + \frac{\delta}{2} & \text{if } \lambda_1 + \frac{\delta}{2} < \lambda_{max} \\ \lambda_2 - \frac{\delta}{2} & \text{else}\end{cases}\end{aligned}$$

In [2] Logvinenko provides more details on the terminology and the inverse calculation.

While it has been shown that the two-transition assumption is not strictly true, it provides a very good approximation to the real object color solid [2], at least for the CIE 1931 2° standard observer, which will be adopted for the rest of this paper. It has also been shown that, for an everywhere positive illuminant, there are no metamers among the optimal reflectance functions. This means that each point on the object-color surface can be uniquely identified by the transition wavelengths λ_1 and λ_2. It is also possible to describe the optimal reflectance functions by a central wavelength λ and a spectral bandwidth δ (see [2]). These have the advantage of providing clear perceptual correlates (see Figure 5), but for computational purposes the transitional wavelengths are more convenient.

Logvinenko represents a color in the interior of the solid as a linear combination between gray and the optimal reflectance function $x_{opt}(\lambda;\lambda_1,\lambda_2)$ lying on the same radius from gray. Gray is the achromatic color stimulus generated by the reflectance spectrum $x_{0.5}(\lambda) = 0.5$, and lies at the center of the solid. The amount of gray in a stimulus is described by the *purity* α, such that the spectrum $x(\lambda) = x_{0.5} + \alpha(x_{opt}(\lambda;\lambda_1,\lambda_2) - x_{0.5}(\lambda))$ is metameric to the described color. Figure 2 shows a cross-section of the object-color solid with the gray center, a color stimulus inside the solid and the optimal stimulus lying on the same radius.

For any set of color descriptors (α,δ,λ), or the equivalent $(\alpha,\lambda_1,\lambda_2)$, the sensor responses can be directly calculated as

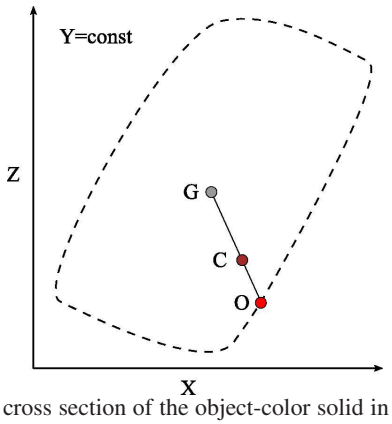

Figure 2: A cross section of the object-color solid in the Y plane showing the gray center (G), a color stimulus inside the solid (C) and the optimal stimulus lying on the same radius (O). The purity α is the relative position of C the on the line connecting G and O: $\alpha = \frac{\text{dist(G,C)}}{\text{dist(G,O)}}$.

$$\begin{aligned} \varphi_i(\alpha,\delta,\lambda) &= \varphi_i(\alpha,\lambda_1,\lambda_2) \quad (1)\\ &= \int_{\lambda_{min}}^{\lambda_{max}} ((1-\alpha)x_{0.5}(\lambda)+\alpha(x_{opt}(\lambda;\lambda_1,\lambda_2))) \\ &\quad s_i(\lambda)I(\lambda)d\lambda \end{aligned}$$

where x_{opt} is the optimal reflectance function defined by λ and δ, s_i are the cone sensitivities, and I is the illuminant.

The subject of this paper is, however, the inverse of this calculation: given a set of sensor responses ψ_i we want to find $(\alpha,\lambda_1,\lambda_2)$ such that

$$\varphi_i(\alpha,\lambda_1,\lambda_2) = \psi_i \quad (2)$$

Since there is no way to invert Equation 1 directly, solving Equation 2 is not trivial.

The paper is organized as follows. Section describes how to obtain the $\alpha\delta\lambda$ coordinates by combining optimization and interpolation; Section presents some results obtained using the new algorithm; and Section concludes the paper.

Calculation of ADL Coordinates by Optimization

Finding the ADL coordinates $\alpha\delta\lambda$ (or the equivalent $\alpha\lambda_1\lambda_2$) corresponding to a set of sensor responses $\vec{\varphi}$ under a given illumination can be approached as an optimization task. The first problem is to find a suitable objective function, that is to say an error measure to be minimized, $E(\alpha,\lambda_1,\lambda_2)$. In agreement with [2] we use the angular error in the sensor space, with the origin at gray, as an error measure. This means we have to calculate the sensor responses $\varphi_i(\alpha,\lambda_1,\lambda_2)$ of the current $\alpha\lambda_1\lambda_2$ (Equation 1), subtract the value of gray from both $\vec{\varphi}_{1,\lambda_1,\lambda_2}$ and $\vec{\varphi}$, and then calculate the angle between them as

$$E(\alpha,\lambda_1,\lambda_2) = \arccos\frac{(\vec{\varphi}-\vec{\varphi}_{0.5})^T(\vec{\varphi}_{1,\lambda_1,\lambda_2}-\vec{\varphi}_{0.5})}{|\vec{\varphi}-\vec{\varphi}_{0.5}||\vec{\varphi}_{1,\lambda_1,\lambda_2}-\vec{\varphi}_{0.5}|} \quad (3)$$

We move the origin to the interior of the solid by subtracting $\vec{\varphi}_{0.5}$, the sensor response of a 50% reflector, in order to obtain non-zero vectors for all colors on the color-solid boundary.

While it is possible to directly minimize E, this is computationally expensive. In [2] it took several days [3] to calculate the ADL coordinates for the set of 1600 glossy Munsell chips (reflectance spectra available at [4]), which makes this method impractical for larger data sets such as spectral images. In order to reduce the time needed for optimization, it is essential to find starting values close enough to the solution. One possible way to find these is to calculate sensor responses for a regular sampling of the ADL space, and then use interpolation to approximate the inverse transformation. However, we have found that interpolation over the whole range of possible $\alpha\lambda_1\lambda_2$ values is computationally expensive. It is thus desirable to restrict the search space, or ideally to reduce its dimensionality.

Obviously the angular error does not depend on the purity α, which correlates to the distance of the stimulus to the origin at gray. This allows us to reduce the search space from three to two dimensions by only considering colors on the color-solid boundary, where $\alpha = 1$. The reduced complexity (computation time reduced from days to minutes) makes it practical to use interpolation to find good starting values for λ_1 and λ_2. Section describes the interpolation process.

Once reasonable starting values have been found, λ_1 and λ_2 can then be obtained as the values minimizing Equation 3 with $\alpha = 1$, giving

$$(\lambda_1,\lambda_2) = \text{argmin}_{\lambda_1,\lambda_2} E(1,\lambda_1,\lambda_2) \quad (4)$$

. Section explains a way to calculate the sensor responses in an efficient manner, allowing for fast optimization. We have used an optimization function for Matlab available on line [5]. In some cases the process does not converge. This can happen, for example, when the illumination spectrum contains sharp peaks. Randomly varying the starting values for the optimization usually solves these problems.

When λ_1 and λ_2 have been found, the purity α can be calculated directly as the relative position of the stimulus on the line connecting the gray center and the optimal stimulus defined by λ_1 and λ_2:

$$\alpha = \frac{|\vec{\varphi}_{1,\lambda_1,\lambda_2}-\vec{\varphi}_{0.5}|}{|\vec{\varphi}-\vec{\varphi}_{0.5}|} \quad (5)$$

In practice, interpolation often yields sufficiently precise results. Optimization is only required in cases where the angular error of the interpolation result is not acceptable. Finally, δ and λ can then be calculated from λ_1 and λ_2. Together, the resulting $\alpha\delta\lambda$ describe a spectrum that is metameric to the stimulus $\vec{\varphi}$ under the given viewing conditions.

Finding starting points by interpolation

Since we consider only colors on the object-color-solid boundary, and the color-solid is a convex volume, we can convert the sensor responses on the boundary into spherical coordinates, discarding the radius and keeping only the spherical angles Θ and ϕ. Firstly, we need to move the origin to the gray center of the color-solid in order to obtain well-defined angles for all points on the boundary, giving

$$\vec{\varphi'} = \vec{\varphi}-\vec{\varphi}_{0.5} \quad (6)$$

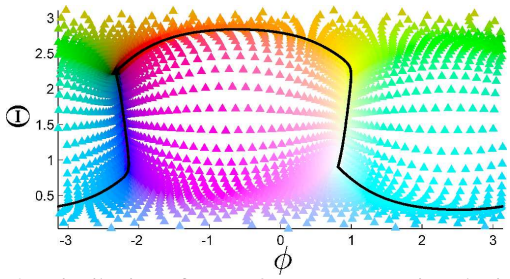

Figure 3: Distribution of Type I/Type II spectra in spherical coordinates. A regular sampling of the wavelength domain in 4 nm steps was used to generate λ_1 and λ_2 values defining the optimal reflectance functions. Illuminant D65 and the CIE 1931 2° observer were used to calculate the sensor responses before converting to spherical coordinates. The black line indicates the boundary between Type I and Type II.

. The spherical angles are calculated as

$$\Theta = \arccos \frac{\varphi'_3}{|\vec{\varphi}'|} \tag{7}$$

$$\phi = \text{atan2}(\varphi'_2, \varphi'_1) \tag{8}$$

We are now looking for a function $F : (\Theta, \phi) \rightarrow (\delta, \lambda)$, which approximates the inverse of Equation 1. Specifically we would like to find λ_1 and λ_2 defining the optimal reflectance function whose sensor responses are on the radius from gray as $\vec{\varphi}$, which means that the spherical angles Θ and ϕ should be identical. Since there are no metamers on the color-solid boundary, there is a one-to-one correspondence between (Θ, ϕ) and (λ_1, λ_2).

At the boundary between Type I and Type II we observe discontinuities in δ and λ (see Figure 4), which can cause problems in the interpolation by generating intermediate values while actually there should be a step. This can be avoided by attempting interpolation for Type I and Type II separately. Figure 3 shows the distribution of Type I and Type II optimal reflectance functions in the spherical coordinate system. The space is evenly divided between the two types, however there is no simple way to determine the type of an arbitrary point in this representation.

Since Type I and Type II reflectances are symmetric with respect to gray, instead of creating separate interpolation functions we can simply calculate the corresponding stimulus value φ^{II} complementary to $\vec{\varphi}$ as

$$\vec{\varphi}^{\text{II}} = \vec{\varphi}_{0.5} - (\vec{\varphi} - \vec{\varphi_{0.5}}) \tag{9}$$

Both $\vec{\varphi^{\text{II}}}$ and $\vec{\varphi}$ can then be converted to spherical coordinates, and we attempt interpolation to find using only Type I reflectances, resulting in 2 possible values for the transition wavelengths, $(\lambda_1^{\text{I}}, \lambda_2^{\text{I}})$ and $(\lambda_1^{\text{II}}, \lambda_2^{\text{II}})$. If the result is better for $\vec{\varphi}^c$, that is to say the angular error in Equation 4 is smaller for $(\lambda_1^{\text{II}}, \lambda_2^{\text{II}})$ than for $(\lambda_1^{\text{I}}, \lambda_2^{\text{I}})$, we are dealing with a Type II reflectance and need to switch λ_1^{II} and λ_2^{II}:

$$(\lambda_1, \lambda_2) = \begin{cases} (\lambda_1^{\text{I}}, \lambda_2^{\text{I}}) & \text{when } E(\lambda_1^{\text{I}}, \lambda_2^{\text{I}}) \leq E(\lambda_1^{\text{II}}, \lambda_2^{\text{II}}) \\ (\lambda_2^{\text{II}}, \lambda_1^{\text{II}}) & \text{else} \end{cases} \tag{10}$$

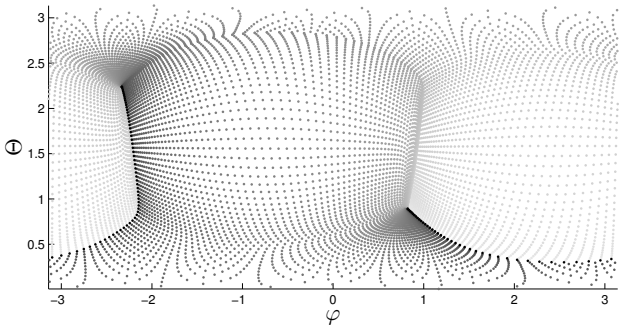

(a) λ_1

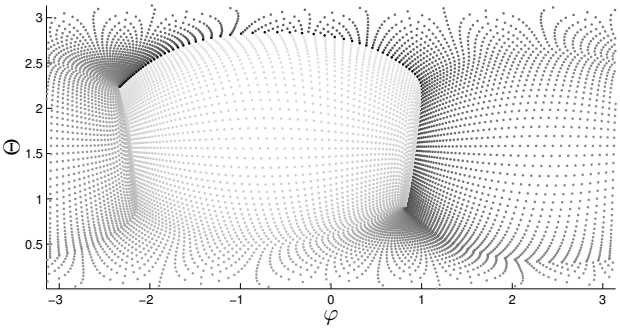

(b) λ_2

Figure 4: The transition wavelengths λ_1 (4a) and λ_2 (4b) for the points in Figure 3. Black represents the lowest possible value (380 nm), and white the highest possible value (780 nm). Note that a change from Type I to Type II occurs when we go from $\lambda_1 \leq \lambda_2$to $\lambda_1 > \lambda_2$, which also happens when one of the wavelengths exceeds the minimum or maximum (black and white in the image).

For interpolation we have used a linear triangulation based method, available in Matlab as TriScatteredInt [6], which performed better than natural neighbor interpolation or radial basis functions (see [1] for a review of scattered data interpolation methods). The interpolation data is created by generating Type I spectra, varying λ_1 and λ_2 in regular steps, and calculating the sensor responses for all of these spectra. We have found that 1 nm steps provide a good compromise between speed and precision. The transition wavelengths can then be converted into spectral bandwidth and central wavelength.

Efficient calculation of sensor responses

The optimization process requires repeated computation of the sensor responses $\vec{\varphi}_{\lambda_1,\lambda_2}$ for optimal reflectance functions $x_{opt}(\lambda;\lambda_1,\lambda_2)$. The sensor responses have the general form

$$\varphi_{\lambda_1,\lambda_2} = \int_{\lambda_{min}}^{\lambda_{max}} x_{opt}(\lambda;\lambda_1,\lambda_2)\vec{s}(\lambda)I(\lambda)d\lambda \tag{11}$$

Since the optimal reflectance functions of Type I (where $\lambda_1 \leq \lambda_2$) only take values of one on the interval $[\lambda_1,\lambda_2]$ and are zero everywhere else, we can rewrite Equation 11 as

$$\vec{\varphi}_{\lambda_1,\lambda_2} = \int_{\lambda_1}^{\lambda_2} \vec{s}(\lambda)I(\lambda)d\lambda \tag{12}$$

. We can now use the antiderivative $\vec{\varphi}(\lambda)$ of the integrand in Equation 12 given by

$$\vec{\varphi}(\lambda) = \int_{\lambda_{min}}^{\lambda} \vec{s}(\lambda')I(\lambda')d\lambda' \tag{13}$$

in order to simplify Equation 12 to

$$\vec{\varphi}_{\lambda_1,\lambda_2} = \vec{\varphi}(\lambda_2) - \vec{\varphi}(\lambda_1) \tag{14}$$

The antiderivative $\vec{\varphi}$ does not depend on the optimal reflectance function. We have precomputed $\vec{\varphi}$ at 0.1 nm steps and interpolated it using splines, so the calculation of sensor responses for an optimal reflectance function now only requires evaluating the spline function at the points λ_1 and λ_2, which is significantly faster than numerical integration.

For Type II optimal reflectance functions (where $\lambda_1 > \lambda_2$) we can calculate the sensor response by exploiting the fact that each Type II spectrum has a complementary Type I spectrum. By definition (see Section 1) the complementary spectra add up to white, and we can calculate the sensor response for a Type 2 reflectance function as the difference between white and the complementary Type I responses:

$$\vec{\varphi}_{\lambda_1,\lambda_2} = \vec{\varphi}(\lambda_{max}) - (\vec{\varphi}(\lambda_1) - \vec{\varphi}(\lambda_2)) \tag{15}$$

Combining Equations 14 and 15 we obtain the following expression for calculating the sensor response of any two-transition optimal reflectance function

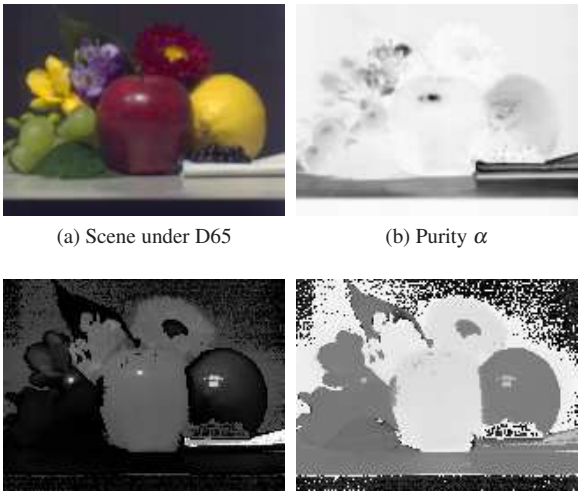

(a) Scene under D65 (b) Purity α

(c) Bandwidth δ (d) Central wavelength λ

Figure 5: The $\alpha\delta\lambda$ color descriptors calculated for a scene under D65. The original XYZ were calculated from the spectral reflectance image based on the CIE 1931 2° standard observer. The maximum angular error threshold (see Equation 3) was set to 0.05°.

$$\vec{\varphi}_{\lambda_1,\lambda_2} = \begin{cases} \vec{\varphi}(\lambda_2) - \vec{\varphi}(\lambda_1) & \text{when } \lambda_1 \leq \lambda_2 \\ \vec{\varphi}(\lambda_{max}) - (\vec{\varphi}(\lambda_1) - \vec{\varphi}(\lambda_2)) & \text{when } \lambda_1 > \lambda_2 \end{cases} \tag{16}$$

This allows for efficient computation of $\vec{\varphi}_{\lambda_1,\lambda_2}$ and significantly speeds up optimization.

Since integration is a linear operation, Equation 16 can also be used to calculate the sensor responses for non-optimal coordinates $\alpha\delta\lambda$, changing Equation 1 to

$$\vec{\varphi}_{\alpha,\delta,\lambda} = \vec{\varphi}_{0.5} + \alpha(\vec{\varphi}_{\lambda_1,\lambda_2} - \vec{\varphi}_{0.5}) \tag{17}$$

which only requires the calculation of sensor responses for optimal reflectance functions.

Results/Discussion

The proposed algorithm is significantly faster than the previous implementation [3]. For the set of 1600 glossy Munsell samples used in [2], with a maximum angular error (see Equation 3) of 0.001°, the calculation now takes roughly 90 seconds instead of several days (Matlab version 2009b running on a Power Mac G5).

Depending on the required precision and the size of the data set, a compromise has to be found between interpolation versus optimization. For large data sets, high-resolution interpolation will yield sufficiently accurate results for many colors, but the creation of the interpolation functions by triangulation quickly becomes too time consuming. For small data sets, it may be faster to use only a low-resolution interpolation and rely on optimization to find the correct $\alpha\delta\lambda$ descriptors. For repeated calculations involving the same illuminant and observer, the interpolation functions need to be calculated only once, and can be stored for reuse.

Figure 5 shows the calculated color descriptors for a scene under D65 (spectral image retrieved from the Joensuu spectral

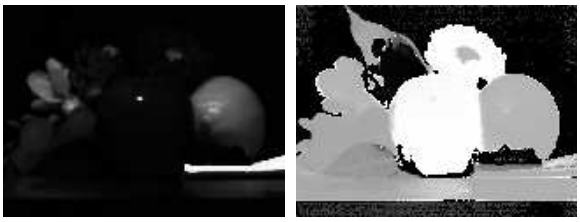

(a) Bandwidth $\tilde{\delta}$ (b) Central wavelength $\tilde{\lambda}$

Figure 6: The reparametrized bandwidth and central wavelength for the scene in Figure 5.

database [4]). We can observe the perceptual correlates of the descriptors as described by Logvinenko. Central wavelength (Figure 5d) is correlated to hue. The spectral bandwidth (Figure 5d) correlates with blackness and whiteness, but becomes meaningless for low purities (gray colors). Purity (Figure 5b) describes the *grayness* of a color, namely, the relative distance to the gray center (see Equation 1). For example, black and white have a high purity, as can be seen in the dark background regions of the image.

The results highly depend on the selected wavelength interval, and it would be useful to normalize the values to a standard range. For this purpose Logvinenko has introduced a reparametrization of the wavelength interval (see [2]), taking into account the magnitude of the sensor responses. For example, the sensor sensitivities at long ($>$ 700nm) and short ($<$ 400nm) wavelengths are very low, and reparametrization compresses these portions of the spectrum. The reparametrized $\alpha\delta\lambda$ descriptors are denoted as $\alpha\tilde{\delta}\tilde{\lambda}$. The purity α is not concerned by reparametrization, since it does not affect the wavelength range determined by the descriptors. Figure 6 shows the reparametrized descriptors corresponding to the image in Figure 5, the results become less dependent on the selected wavelength range, and the descriptors are more consistent across uniform regions of the image.

One of the possible applications of ADL color descriptors is the prediction of the effect of an illumination change. Since the colors are now essentially described by a reflectance spectrum, we can simply calculate the sensor response (camera RGB or cone LMS) for any given illuminant according to Equation 1. Figure 7 shows the result obtained by calculating the RGB sensor responses for the color descriptors in Figure 5, using CIE illuminant A instead of D65. Errors in the prediction are a result of the illuminant-induced color-stimulus shift described by Logvinenko [2]. Although the ADL *space* is invariant to illumination, the $\alpha\delta\lambda$ *color descriptors* themselves can change with the illumination, since each $\alpha\delta\lambda$ triplet describes a class of metamers, and metamerism depends on the illuminant.

Using the proposed algorithm we also investigate the illuminant-induced shift in the color descriptors for less smooth illuminants, including fluorescent ones. Figures 8-10 show the color stimulus shift for an illumination change from D65 to F11, which is clearly different from, and larger than, the shift induced by changing from D65 to A. The significant differences in the illuminant spectrum create the larger shifts in spectral bandwidth

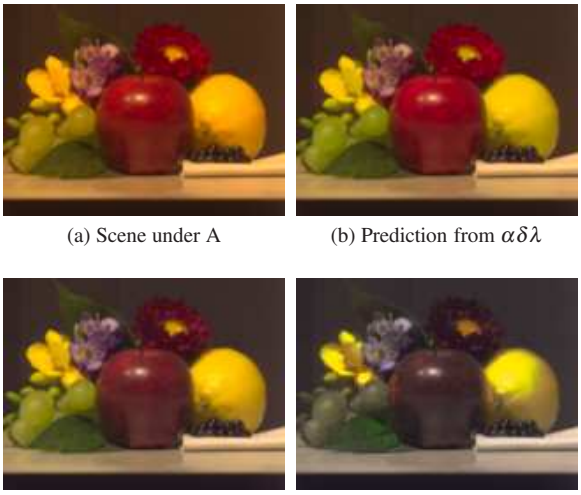

(a) Scene under A (b) Prediction from $\alpha\delta\lambda$

(c) Scene under F11 (d) Prediction from $\alpha\delta\lambda$

Figure 7: The prediction of illumination change from D65 to A and F11. On the left the result calculated from the original spectral image, and on the right the result obtained by relighting the color descriptors (calculated from the scene illuminated D65) with illuminant A and F11.

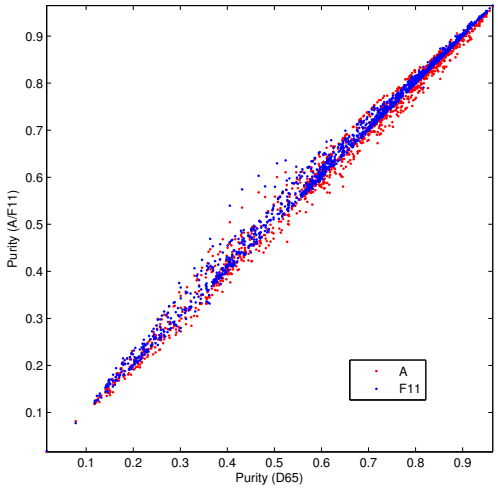

Figure 8: The illuminant-induced shifts for the 1600 glossy Munsell chips in purity. The reference illuminant is D65 and test illuminants are A (red) and F11 (blue).

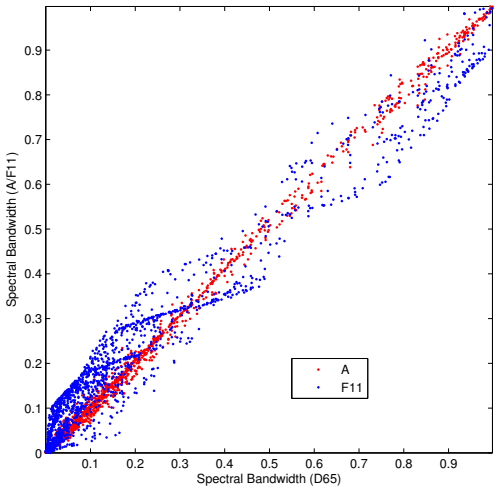

Figure 9: The illuminant-induced shifts for the 1600 glossy Munsell chips in reparametrized spectral bandwidth $\tilde{\delta}$. The significant differences in the illuminant spectrum create a larger effect for F11, which is a fluorescent light with narrow peaks in the power distribution.

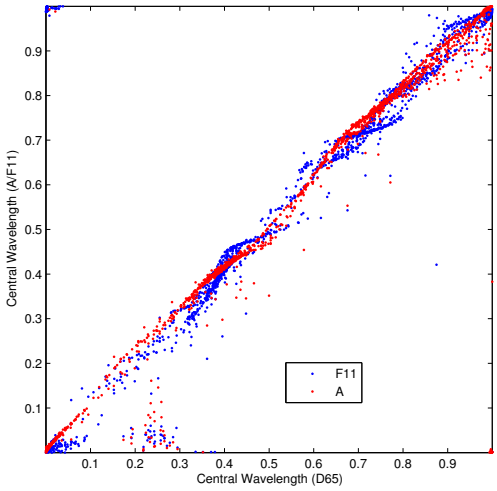

Figure 10: The illuminant-induced shifts for the 1600 glossy Munsell chips in reparametrized central wavelength $\tilde{\lambda}$.

(Figure 10) and central wavelength (Figure 8) for F11, which is a fluorescent light with narrow peaks in the power distribution. Purity (Figure 8) seems to be least affected by an illumination change.

Conclusion

The proposed algorithm provides a significant decrease in computation time compared to the existing implementation, and enables the calculation of $\alpha\delta\lambda$ color descriptors for a wide range of illuminants, including fluorescent ones that have previously proved problematic. It is now feasible to calculate the descriptors for large data sets or images, clearly visualizing the perceptual correlates of the $\alpha\delta\lambda$ descriptors. This is the first step on the way towards using Logvinenko's object-color space as a device-independent color space in a variety of applications including device characterization and calibration.

References

[1] I. Amidror. Scattered data interpolation methods for electronic imaging systems: a survey. *Journal of Electronic Imaging*, 11:157–176, April 2002.

[2] Alexander D. Logvinenko. An object-color space. *J. Vis.*, 9(11):1–23, 10 2009.

[3] Alexander D. Logvinenko. Private communication, 2010.

[4] University of Joensuu Color Group. Spectral database. http://spectral.joensuu.fi/index.php?page=spi (retrieved: May 2010).

[5] Rody Oldenhuis. Optimize for matlab. http://www.mathworks.com/matlabcentral/fileexchange/24298-optimize (retrieved: May 2010).

[6] The Mathworks. *Matlab User's Guide*. The Mathworks, 2009.

[7] Günther Wyszecki and W. S. Stiles. *Color Science: Concepts and Methods, Quantitative Data and Formulae*. Wiley-Interscience, 2 edition, August 2000.

Author Biography

Christoph Godau received his B.Sc. in physics from the Ruhr-University Bochum, Germany (2008) and his M.Sc. in Color Science from the University of Saint-Etienne, France, and the University of Eastern Finland (2010). He is a research engineer and Ph.D. candidate at the Center for Mathematical Morphology in Fontainebleau, France.

Brian Funt received the Ph.D. degree in computer science from the University of British Columbia, Vancouver, BC, Canada, in 1976. He is a Professor with the School of Computing Science, Simon Fraser University, Vancouver, where he has been since 1980. He has published widely in color, color constancy, retinex, color calibration, and illumination estimation.